ISSN 1547-4771, Physics of Particles and Nuclei Letters, 2021, Vol. 18, No. 1, pp. 19–26. © Pleiades Publishing, Ltd., 2021.
Russian Text © The Author(s), 2021, published in Pis'ma v Zhurnal Fizika Elementarnykh Chastits i Atomnogo Yadra, 2021.

PHYSICS OF ELEMENTARY PARTICLES AND ATOMIC NUCLEI. EXPERIMENT

Multinucleon Transmissions in ^{18}O (35 MeV/Nucleon) + ^{181}Ta (^{9}Be) Reactions

A. G. Artyukh[a], *, A. N. Vorontsov[a], S. A. Klygin[a], G. A. Kononenko[a], Yu. M. Sereda[a], and B. Erdemchimeg[a, b]

[a] *Joint Institute for Nuclear Research, Dubna, Russia*
[b] *Mongolian State University, Center for Nuclear Research, Ulaanbaatar, Mongolia*
**e-mail: artukh@jinr.ru*

Received July 27, 2020; revised August 10, 2020; accepted August 11, 2020

Abstract—The velocity, charge, and isotopic distributions of the products of nuclear reactions with $2 \le Z \le 11$ have been studied in combinations of ^{18}O (35 MeV/nucleon) + ^{181}Ta (^{9}Be) with a different isotope spin. The correlation of the isotope yields for the detected light elements with value Qgg has been established. The cross sections for the formation of neutron-rich nuclei have been measured and their yields in reactions with different neutron skin have been compared. A qualitative interpretation of the phenomenon of a significant increase in the probability of the formation of neutron-rich nuclei of light elements in reaction ^{18}O (35 MeV/nucleon) + ^{181}Ta in comparison with ^{18}O (35 MeV/nucleon) + ^{9}Be obtained in the reactions with the removal of a proton from the projectile nucleus has also been presented.

DOI: 10.1134/S1547477121010027

INTRODUCTION

Studies of the yields of products with an anomalous N/Z ratio in reactions with heavy ions have shown [1] that multinucleon transfer reactions are an effective means of obtaining neutron-rich nuclei, including nuclei with a maximum neutron excess. In peripheral transfer reactions at low energies, it has been shown that the yield of exotic nuclei on heavy targets (high isotope spin) demonstrates a significant increase in comparison with the yields on light targets (low isotope spin). At the same time, the study of the yields of neutron-rich nuclei at high energies [2] does not show a noticeable increase in the yields on targets with an increase in the isotope spin of the target nucleus. Based on model calculations, the author of [3] concludes that the features observed in the yields of neutron-rich nuclei with collision energies are apparently due to variations in the contributions of the scattering cross sections of individual n–p, n–n, and p–p channels to the formation of product yields with an anomalous N/Z ratio.

The noted features of transfer reactions in peripheral nucleus–nucleus collisions stimulated the setting up of experiments with ^{18}O ion beams with energy in the Fermi energy range (~37 MeV/nucleon for stable nuclei) on target nuclei with different isotope spins.

1. EXPERIMENTAL STUDIES OF THE CHARACTERISTICS OF NUCLEAR REACTIONS IN THE TRANSITIONAL ENERGY REGION (FERMI ENERGY REGION)

The experiments were carried out with ^{18}O ion beams (35 MeV/nucleon) using a ^{9}Be target (thickness of 14 mg/cm^2) and targets with high ^{181}Ta isotope spin (thickness of 14 mg/cm^2). The identification (by A and Z) and measurement of velocity distributions were performed using a KOMBAS fragment separator [4]. The technical details of the experiments are detailed in [5].

The results of measurements of the rate distributions of products obtained in reactions ^{18}O (35 MeV/nucleon) + ^{181}Ta (^{9}Be) are presented in Fig. 1. For both reactions, the data demonstrate a strong asymmetry of the contributions from reactions of nucleon stripping from a projectile nucleus when compared to pickup reactions.

Figure 1 also shows that

(1) velocity distributions obtained on more neutron-rich target ^{181}Ta are narrower than the light ^{9}Ve target. This may indicate a less dissipative nature of the formation of registered projectile-like products in the ^{18}O + ^{181}Ta reaction. As a result, the contribution of the low-speed component to their integral output becomes smaller;

(2) for a light target, a more significant broadening of the velocity spectra is observed with a decrease in mass number A of the isotope, as well as with a decrease in the atomic number Z of the element. The bell-shaped spectrum observed for the most neutron-rich isotopes also broadens towards lower velocities;

(3) for both reactions, there is a drift of the maxima of the rate distributions to lower rates for the products obtained in exchange reactions (for example ^{18}C($-2p$, $+2n$),^{18}N ($-1p$, $+1n$)) and the products obtained by picking up neutrons and protons;

(4) for the products obtained in the reactions of only the stripping of nucleons from the projectile

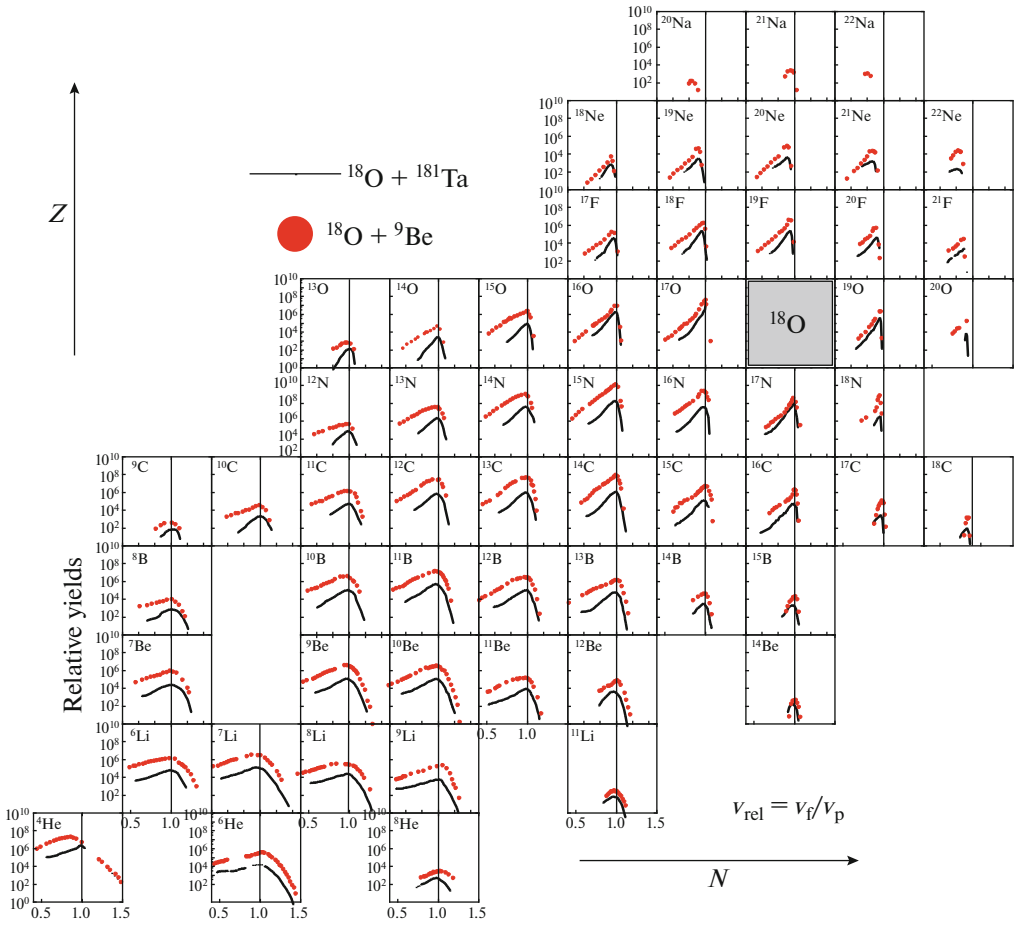

Fig. 1. View of velocity distributions of isotopes of the lightest and lightest elements obtained in two reactions ^{18}O (35 MeV/nucleon) + ^{181}Ta (^{9}Be). The vertical lines dissecting the cells show velocities V_{beam} of ^{18}O.

nucleus, the maxima of the velocity distributions coincide with the velocity of the projectile nucleus.

In comparison with the characteristics of the velocity distributions obtained at low collision energies [1], in the studied range of intermediate energies (35 MeV/nucleon), qualitative changes are observed in the spectra of products obtained mainly in nucleon stripping. Namely, despite the multinucleon nature of the transfer reactions leading to the formation of neutron-rich product nuclei in both nuclear reactions (Ta and Be targets), their maxima are concentrated at speeds comparable to those of the projectile nucleus. In nuclear reactions at low energies of bombarding particles, the observed property is a characteristic leash for quasi-elastic low-nucleon transfers.

Figure 2 shows the isotopic A distributions for each atomic number–product obtained in the reactions ^{18}O (35 MeV/nucleon) + ^{9}Be (^{181}Ta). The experimental isotope distributions were obtained by integrating the isotope velocity distributions in the measured velocity range for each element. The contribution to the A distribution of ^{18}O product–isotope yields is excluded due to the impossibility of correctly separating them from the contribution of the initial ^{18}O projectile nucleus.

It can be seen from Fig. 2 that the mass distributions for each element, with the exception of helium, have similar wide bell-shaped forms for both reactions, with maxima corresponding to the mass number A of the stable isotope.

Figure 3 shows the elemental Z distributions of products obtained in reactions of ^{18}O oxygen ions (35 MeV/nucleon) on two targets, ^{9}Be and ^{181}Ta. The experimental charge distributions were obtained by integrating the yields of measured isotope distributions for each element. For both reactions, the experimental elemental distributions demonstrate a similar nature of the dependence with broad maxima in the region of atomic number Z of the projectile nucleus. There is a sharp decline in the yields of products with atomic numbers greater than Z of the projectile nucleus and an increase in the yields of the lightest elements with $Z \leq 3$.

Figure 4 shows the distributions of the yields of isotopes of the lightest and light elements presented,

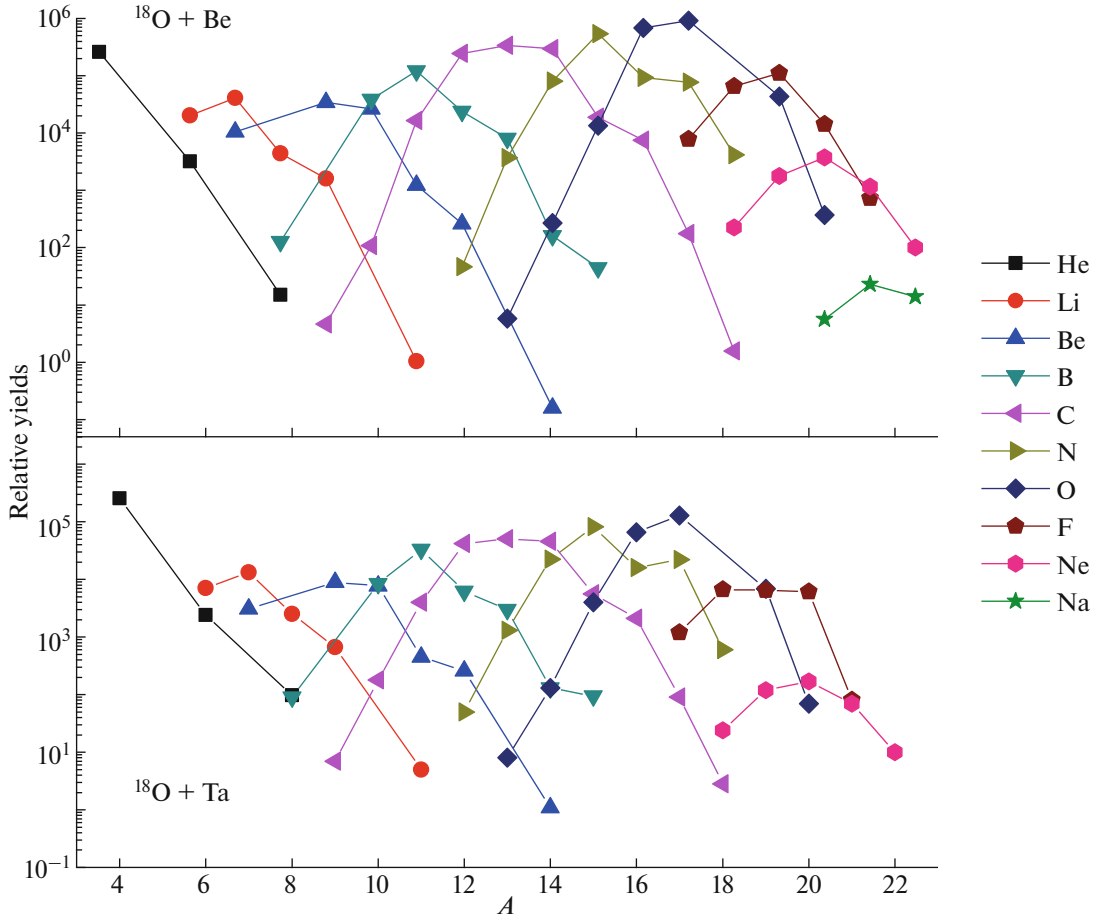

Fig. 2. Comparison of mass (A distribution) spectra of projectile-like products studied in two nuclear reactions at intermediate energy ^{18}O (35 MeV/nucleon) + ^{9}Be (^{181}Ta).

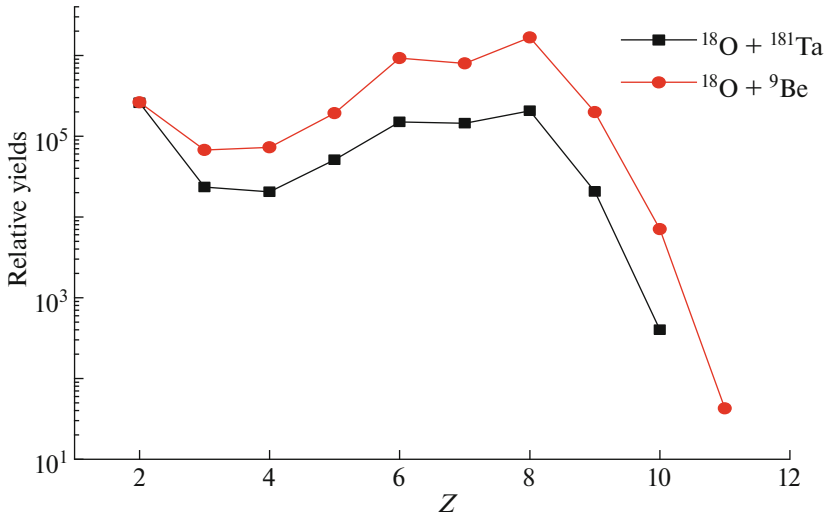

Fig. 3. Comparison of charge (Z distribution) spectra of projectile-like products of nuclear reactions obtained in two reactions ^{18}O (35 MeV/nucleon) + ^{9}Be (^{181}Ta) with different neutron skins.

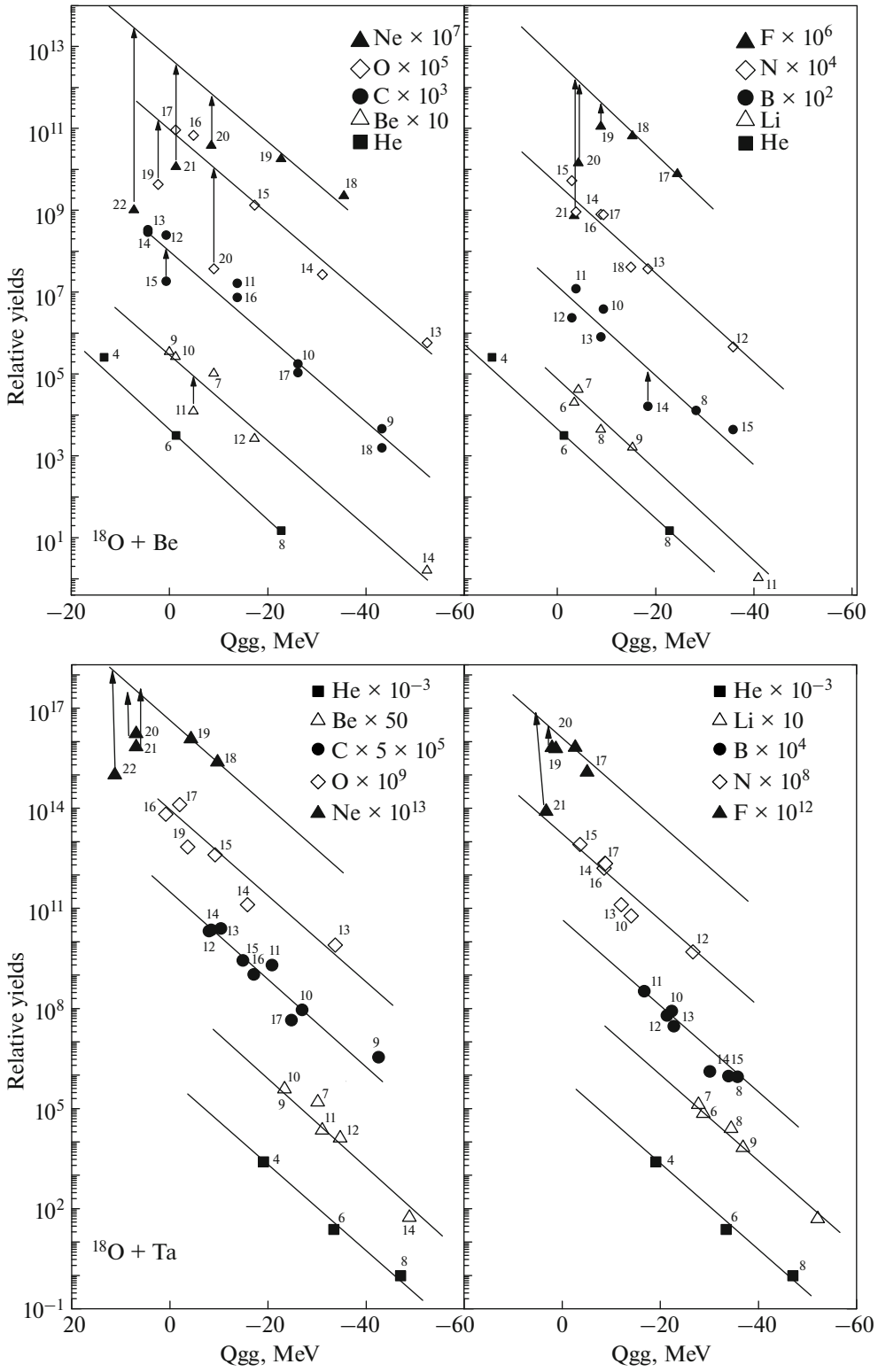

Fig. 4. Qgg taxonomy of the yields of projectile-like products of nuclear reactions obtained in combinations ^{18}O (35 MeV/nucleon) + ^{9}Be and ^{18}O (35 MeV/nucleon) + ^{181}Ta.

depending on the energy consumption for their formation (systematics of the yields of cold nuclei Qgg). The observed formation of cold nuclei and their survival under the conditions of such a deep rearrangement of the initial partners can be understood if we assume that they are products of the elastic exchange of nucle-

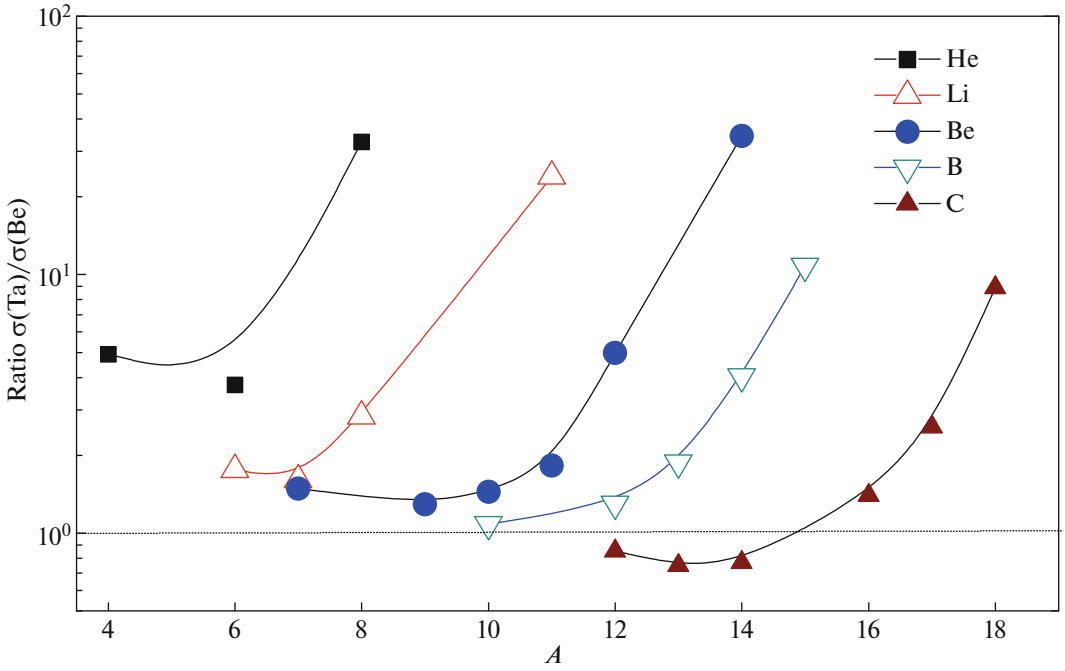

Fig. 5. Ratio of the cross sections for the formation of neutron-enriched projectile-like isotopes for the light elements He, Li, Be, B, and C obtained in reactions ^{18}O (35 MeV/nucleon) + ^{181}Ta (^{9}Be).

ons between the participants of the reaction (with zero excitation).

Figure 5 shows a comparison of the cross sections for the production of mainly neutron-rich isotopes obtained in the two reactions studied. As can be seen from the figure, the enrichment of the contact zone with a neutron excess of the target in the reaction ^{18}O + ^{181}Ta leads to a noticeable increase in the cross section for the formation of extremely neutron-rich product nuclei, especially isotopes at the nucleon stability boundary. As follows from the Qgg systematics (Fig. 4), these nuclei are obtained in the processes of removing many protons from the projectile nucleus, leaving both reaction partners cold.

Such a noticeable effect of additional neutrons in the contact zone on the efficiency of the formation of projectile-like neutron-rich nuclei obtained in the reactions of removing protons from a projectile nucleus may indicate [3] the increasing contribution of quasi-free n–p scattering channel compared to n–n and n–p channels in agreement with a functional dependence of free scattering, as is shown in Fig. 6 [3, 6].

From the functional dependence of the scattering of free nucleons (Fig. 6), it is seen that, in the energy range of up to 200 MeV/nucleon, n–p channel scattering exceeds p–p and n–n channels in intensity by more than three times. The higher probability of n–p scattering compared to components n–n and p–p promotes the more active removal of protons from the projectile nucleus ^{18}O, which is observed in the advantage of the yields of projectile-like nuclei in the studied pair of reactions. An alignment of elastic scattering cross sections at high bombarding energies for channels n–p, n–n, and p–p, confirms the attenuation of advantages of the n–p channel observed in experiments [2].

2. MODEL QMD ANALYSIS OF EXPERIMENTAL DATA

To simulate the characteristics of peripheral processes in the studied reactions in the Fermi energy range, the Quantum Molecular Dynamics (QMD) model [7–9] and the computational code implemented on its basis [10] were used. An extended QMD model analysis is presented in [11].

Figures 7a and 7b show the results of a simulation of charge distributions for a series of ranges of collision impact parameters (as they increase), as well as a model calculation for the full range of collision parameters for both reactions. To react on the ^{9}Be light target, simulations were performed over the full range of collision parameters b = 0–6 fm ($R_{proj} + R_{tar}$ = 5.36 fm), and for the ^{181}Ta heavy target, in the range b = 0–10 fm ($R_{proj} + R_{tar}$ = 9.44 fm), respectively.

From model estimates for the ^{18}O (35 MeV/nucleon) + ^{181}Ta (forward kinematics) heavy target shown in Fig. 7a, it follows that the calculation predicts the partial contribution of different ranges of impact parame-

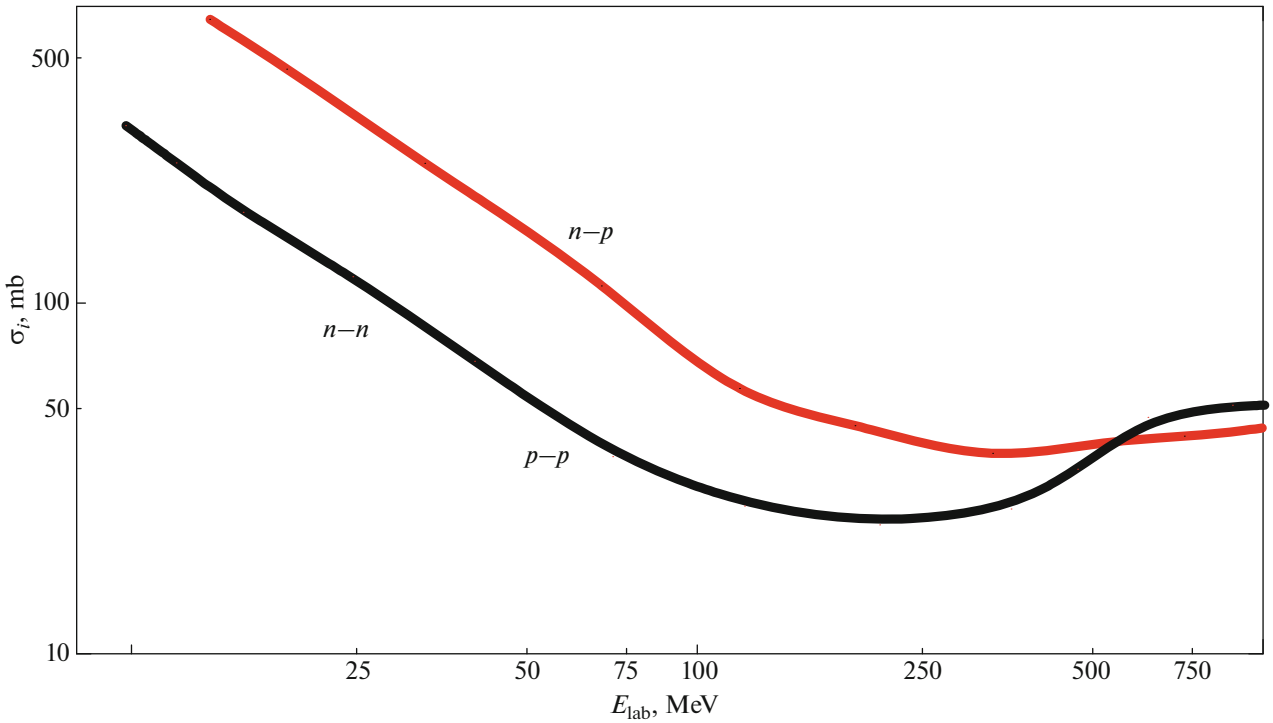

Fig. 6. Cross sections of free nucleon–nucleon collisions versus energy in laboratory coordinate system [3, 6].

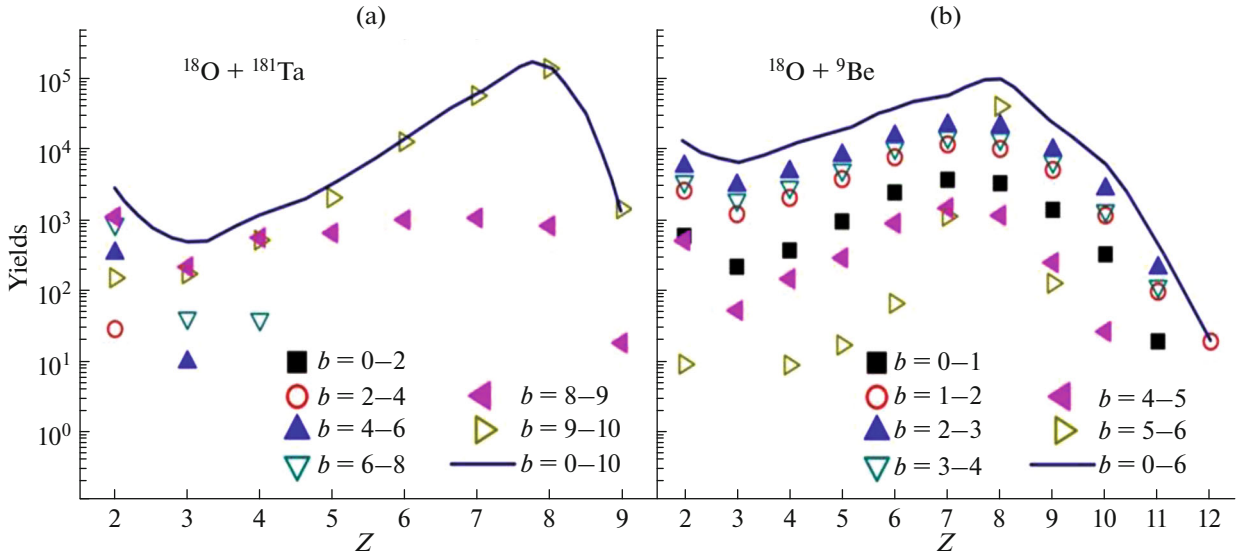

Fig. 7. Evolution of the shape of charge distributions depending on the value of the impact parameters of the collision for two combinations of projectile-target: (a) ^{18}O (35 MeV/nucleon) + ^{181}Ta and (b) ^{18}O (35 MeV/nucleon) + ^{9}Ve. The solid line indicates the shape and positions of the maxima of the model charge distributions of nuclear reaction products over the full ranges of impact parameters.

ters to the yield of products, both with atomic numbers near and above the atomic number of the projectile nucleus and in the region of the lightest elements. Thus, products with atomic numbers $Z \geq 5$ are formed mainly in peripheral collisions with $b \geq 8$ fm, while the group of lightest elements with $Z_{frag} = 2, 3, 4$ is formed in collisions with impact parameters $b = 2$–8 fm (closer to the central one).

For the $^{18}O + ^{9}Be$ (inverse kinematics) light system shown in Fig. 7b, it can be seen that products are

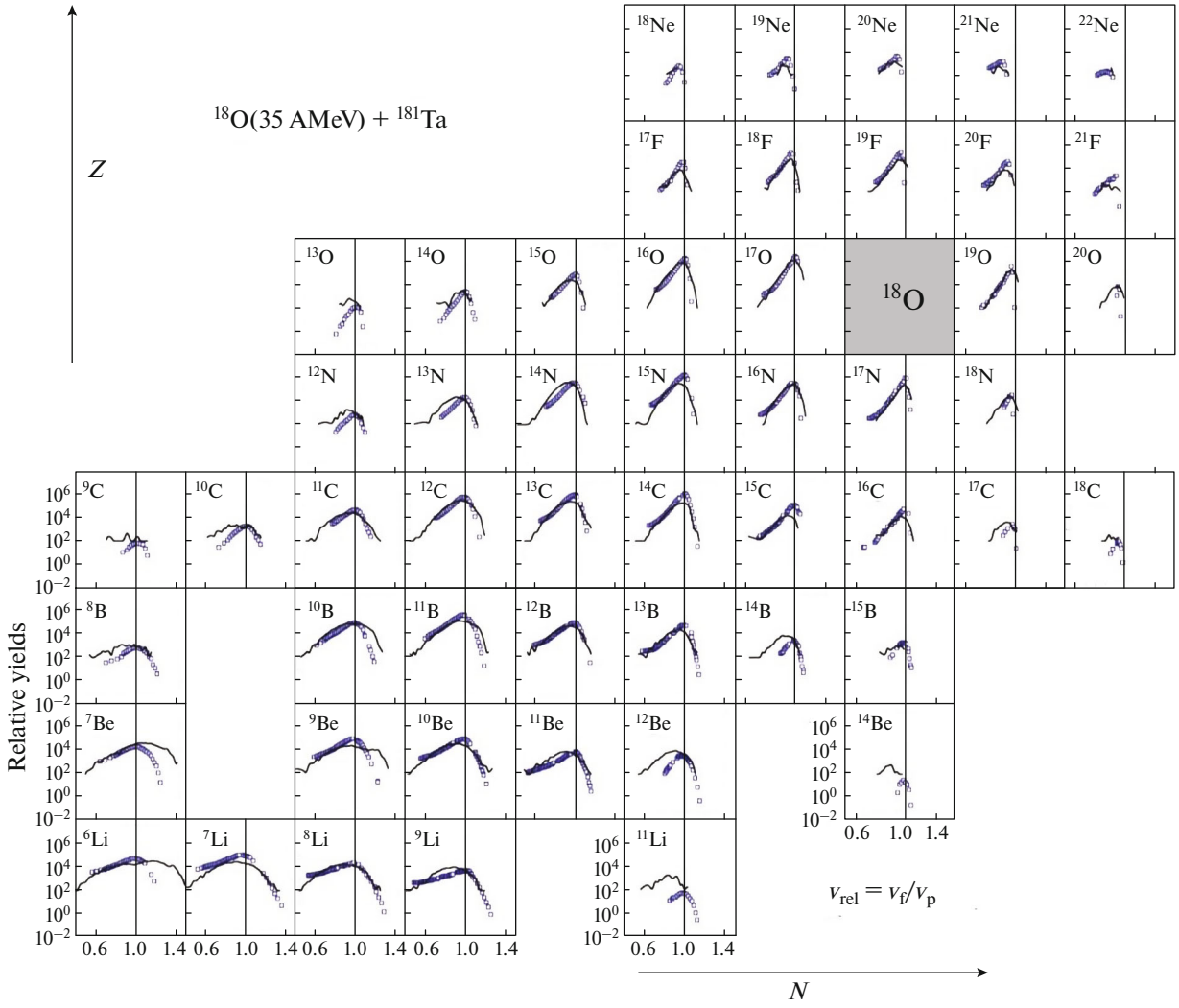

Fig. 8. Comparison of experimental (filled circles) with model (thin lines) relative velocity distributions for isotopes of the measured series of products of light elements with $Z = 3–10$ studied in reaction ^{18}O (35 MeV/nucleon) + ^{181}Ta. For the sake of clarity, the values of the positions of the maxima of the experimental and calculated distributions are aligned on the ordinate scale. The solid line vertically dissecting cells [Z, A] shows velocities V_{beam} of the ^{18}O beam.

formed mainly in collisions characterized by the range of collision parameters $b = (1–4)$ fm. In this case, the interval of central collisions ($b = 0–1$ fm) forms a minimum contribution to the integral charge distribution, nevertheless repeating the behavior of the shape of the charge distribution without any changes. In model estimates, a minimum is observed in the yields of products at $Z = 3$, while in the region $Z = 4–8$ there is a tendency for a smooth increase in the yield followed by a rapid decline for $Z > Z$ of the projectile nucleus. Products with $Z = 12$ correspond to the element of complete fusion of the ^{18}O projectile and ^{9}Be target. The small magnitude of such a process, apparently, indicates the low probability of merging of partners at a collision energy of 35 MeV/A.

Figure 8 shows, as an example, comparisons of the calculated results with experimental velocity distributions ($v_{rel} = v_{frag}/v_{proj}$) for the measured series of isotopes of light elements with $Z = 3–10$ obtained in the reaction ^{18}O (35 MeV/A) + ^{181}Ta.

Figure 8 shows that the widths and positions of the maximums of the velocity distributions for the ^{18}O (35 MeV/nucleon) + ^{181}Ta heavy system is satisfactorily reproduced by model calculations, except for the heaviest (neutron-rich) isotopes Li, Be, B, and C, for which the calculated positions of the maxima drift to lower velocities than the measured ones; i.e., the inelasticity of the calculated spectra is exaggerated. For light proton-excess isotopes Be, B, N, and O, the variance of the calculated distributions increases in comparison with the measured ones.

The QMD model calculation of experimental mass and charge distributions satisfactorily reproduces both the shape and position of the maxima [11].

CONCLUSIONS

Disagreements between the QMD model analysis and the experimental velocity distributions (the most representative characteristic of the processes under study), apparently, indicate a significant flaw in the choice of the nuclear interaction potential. The Skyrme potential used in the model is not able to reproduce the experimentally observed and more effective effect of the neutron component in the contact zone of interacting partners, namely, an increase in the yield of neutron-enriched fragments when using a ^{181}Ta target with a higher isotope spin. To adequately take into account the factor of the observed enhancement of the yields of neutron-rich nuclei (Fig. 5) obtained in the reactions of elastic removal of protons (Qgg factor, Fig. 4) from the target nucleus, apparently, a restructuring of the foundations of the nuclear potential will be required. A realistic potential must inevitably take into account the transformation of nucleon–nucleon collisions into quasichannels n–p, n–n, and p–p scattering (Fig. 6) in conditions of low density in the contact zone of partners.

Significant difficulties with the realistic predictions obtained in model approaches are related to the lack of reliable experimental data. To create an adequate theory of this process, systematic experimental studies are required in a much wider range of changes in the N/Z interacting partners and their energies, in which it would be possible to trace the dynamics of the transformation of nucleon–nucleon collisions in peripheral reactions between complex nuclei.

REFERENCES

1. V. V. Volkov, *Treatise on Heavy-Ion Science,* Ed. by D. A. Bromley (Plenum, New York, 1984), Vol. 8, p. 101; V. V. Volkov, "Deep inelastic transfer reactions—the new type of reactions between complex nuclei," Phys. Rep. **44**, 93–157 (1978).
2. C. K. Gelbke, C. Olmer, et al., "Energy dependence of peripheral reactions induced by heavy ions," Phys. Rep. **42**, 311 (1978).
3. B. G. Harvey, "A microscopic calculation of fragment formation in nucleus-nucleus collisions," Nucl. Phys. A **444**, 498–518 (1985); S. E. Koonin, "One-body nuclear dynamics," in *Proceedings of the International School of Physics Enrico Fermi, Varenna, Lake Como, 1979,* pp. 233–259.
4. A. G. Artukh, G. F. Gridnev, et al., "Wide aperture kinematic separator COMBAS realized on the strong focusing principle," Nucl. Instrum. Methods Phys. Res., Sect. A **426**, 605–617 (1999).
5. A. G. Artukh, G. F. Gridnev, et al., "Forward-angle yields of $2 \le Z \le 11$ isotopes in the reaction, of ^{18}O (35 a MeV) with Be," Phys. At. Nucl. **65**, 393–399 (2002).
6. N. J. di Giacomo et al., "Pauli blocking and Fermi motion effects in ion-ion collisions," Phys. Lett. B **101**, 383–386 (1981).
7. J. Aichelin and G. F. Bertsch, "Numerical simulation of medium energy heavy-ion reactions," Phys. Rev. C **31**, 1730–1738 (1985).
8. G. F. Bertsch and S. Das Gupta, "A guide to microscopic models for intermediate energy heavy-ion collisions," Phys. Rep. **160**, 189–233 (1988).
9. J. Aichelin, "Quantum molecular dynamics—dynamical microscopic N-body approach to investigate fragment formation and the nuclear equation of state in heavy-ion reactions," Phys. Rep. **202**, 233–360 (1991).
10. J. Lukasik and Z. Majka, "CHIMERA (Microscopic approach to heavy ion collisions at intermediate energies)," Acta. Phys. Polon., B **24**, 1959–1980 (1993).
11. A. G. Artukh et al., "QMD approach in description of the ^{18}O + ^{9}Be and ^{18}O + ^{181}Ta reactions at $E_{proj} = 35$ A MeV," Acta Phys. Polon. B **37**, 1875–1892 (2006).